Available online at www.sciencedirect.com
SCIENCE DIRECT®
Journal of the European Ceramic Society 25 (2005) 401–406
www.elsevier.com/locate/jeurceramsoc

Analysis of secondary phases segregated and precipitated in SnO_2-based varistors

R. Parra [a,*], M. S. Castro [a], J. A. Varela [b]

[a] *Institute of Materials Science and Technology INTEMA, CONICET-UNMdP, J.B. Justo 4302, B7608FDQ Mar del Plata, Argentina*
[b] *Instituto de Química, UNESP, P.O. Box 355, 14801-970 Araraquara, SP, Brazil*

Received 16 October 2003; received in revised form 12 February 2004; accepted 25 February 2004
Available online 21 July 2004

Abstract

Transmission and scanning electron microscopy techniques were used to study the heterogeneities found in the microstructure of SnO_2·Co_3O_4·Nb_2O_5·Fe_2O_3 and SnO_2·ZnO·Nb_2O_5·Fe_2O_3 varistors. Second phases encountered both inside the grains and in grain boundary regions were identified using energy dispersive spectrometry and electron diffraction patterns. Through the electrical characterisation, the presence of iron oxide among the additives was determined to highlight the non-linear properties of the specimens. A discussion on the influence of second phases on the non-linear features of these systems is also addressed.

Keywords: Electron microscopy; Grain boundaries; Microstructure-final; Varistors; SnO_2

1. Introduction

Metal oxide varistors are electronic ceramic devices whose function is to sense and limit transient voltage surges and to do so repeatedly without being destroyed or damaged.[1,2] They can be used over wide ranges of voltages and currents according to their specific properties.[3]

Varistors are often prepared by mixing oxides of the desired composition and subjecting the powder to conventional techniques of pressing and sintering. When the sintering is complete, the resultant product is a polycrystalline ceramic with a grain boundary property that contributes to the well known, yet most important, characteristic of the device: its non-linear *I–V* behaviour. The non-linearity is a grain boundary phenomenon where a barrier to majority of carriers (electrons) exists in the depletion layer of adjacent grains. The negative surface charge at the grain boundary interface is compensated by the positive charge in the depletion layer in the grain on both sides of the interface. Thermionic emission and tunnelling are acknowledged to be the major transport mechanisms.[3,4]

The SnO_2-based varistor system doped with ZnO or with Co_3O_4 presents a simple single phase structure under X-ray resolution in which Sn^{4+} ions are substituted by Zn^{2+}, Co^{3+} or Co^{2+} ions giving place to a solid solution, as already discussed in the literature.[5,6] However, the existence of a Co enriched second phase has been suggested by Oliveira et al.[7] on SnO_2·CoO-based varistors sintered at 1250 °C for 2 h using transmission electron microscopy. Furthermore, these heterogeneities localised mainly at grain boundaries and triple points, are not only rich in Co but also in the dopant elements eventually added to improve the non-linearity coefficient. This enrichment of grain boundaries with precipitates and segregated species is likely to control the non-ohmic properties of the devices.[8,9]

The purpose of the present work is to characterise the second phases observed by scanning electron microscopy (SEM) and transmission electron microscopy (TEM) in SnO_2-based varistors, their microstructure and composition, their influence on the global microstructure development and how they might modify the electrical behaviour of these devices.

2. Experimental procedure

Analytical grades of SnO_2 (Aldrich, 99.9%, −325 mesh, BET determined specific surface area of 5.5 $m^2\ g^{-1}$), Co_3O_4 (Merck, >99%), ZnO (Baker, >99%), Nb_2O_5 (Fluka AG,

* Corresponding author.
E-mail address: rparra@fi.mdp.edu.ar (R. Parra).

0955-2219/$ – see front matter © 2004 Elsevier Ltd. All rights reserved.
doi:10.1016/j.jeurceramsoc.2004.02.010

Table 1
Sample composition (mol%)

	SnO_2	ZnO	Co_3O_4	Nb_2O_5	Fe_2O_3
SCNF	99.595	–	0.330	0.025	0.050
SZNF	98.925	1.00	–	0.025	0.050

99.9%) and Fe_2O_3 (Baker, >99%) were used as precursors for processing SnO_2-based varistors. Selected compositions are listed in Table 1. Starting powders were mixed in an alcoholic medium by stirring in a high-speed turbine at 6000 rpm for 5 min and subsequently dried at 65 °C until constant weight. After being cooled down, mixtures were crushed into powders and sieved through a 43 μm mesh screen. In order to obtain discs of a thickness around 1 mm, powders were uniaxially pressed at 80 MPa, stage followed by an isostatic pressing at 200 MPa. Finally, samples were sintered in air at 1300 °C for 2 h with heating and cooling rates of 3 °C min^{-1}.

The apparent density of the sintered samples was determined applying the Archimedes method. X-ray powder diffraction (XRD) analysis was carried out by means of a Rigaku 22000 equipment running with Cu Kα radiation.

The microstructures were characterised by SEM in a Topcon SM-300 microscope under the secondary electrons mode, and by TEM in a Philips CM200 instrument operating at 200 kV.

Sample preparation for SEM consisted in polishing with SiC paper and diamond pastes; a 15 min thermal etching 50 °C below the sintering temperature was finally performed. Suitable samples for TEM were prepared by cutting discs of plane and parallel faces of 3 mm in diameter using an ultrasonic cutter. The discs were grinded down to a thickness of 100 μm and then dimpled by means of an SBT Dimple Grinder Model 515 to get a 30 μm thickness at the centre of the specimens. Finally, to obtain large electron transparent regions, ion milling was performed using a Bal-Tech RES010 ion mill operating at 4 kV and 1.5 mA on each gun. Electron diffraction patterns were obtained from selected areas as an aid to identify the different phases found in the microstructures. The fundamental relationship in a diffraction pattern

$$Rd = \lambda L, \quad (1)$$

where R is any distance measured on the pattern related to a specific d spacing in the crystal and $\lambda L = 2.32 \times 10^{-12}$ m^2 is the microscope constant, was applied.[10]

Both SEM and TEM instruments were equipped with EDS (PGT PRISM-Digital Spectrometer) systems, operating at acceleration voltages of 30 and 200 kV, respectively, for energy dispersive X-ray analysis.

The sintered samples were lapped to ensure plane parallel faces where silver electrodes were deposited for electrical characterisation. A Keithley 237 high voltage source-measure unit was used to acquire room temperature plots of the current density as function of the electric field.

Table 2
Densities, mean grain sizes and non-linearity coefficient of samples sintered at 1300 °C for 2 h

Sample	Density (g cm^{-3})	Relative density (%)	d (μm)	α
SCNF	6.84	98.4	6.9	25
SZNF	6.79	97.7	2.3	9

3. Results and discussion

From the XRD analysis only peaks corresponding to SnO_2 were detected; no other crystalline phase besides cassiterite (SnO_2) was observed, indicating apparently single-phase systems within the detection limits of X-ray diffraction.

Table 2 shows the densities and mean grain sizes of the sintered samples; the former were obtained through the Archimedes method and the latter through the method of the intercepts proposed by Mendelson.[11] Fig. 1 shows the SEM microstructure of the SCNF system whereas Fig. 2 shows that corresponding to the SZNF system. Although both images were recorded from polished samples, it was decided not to carry out the usual Au coating on sample SZNF; then, a higher acceleration voltage was needed to achieve an acceptable image resolution. According to the oxides added and to the types of defects they give rise to, different sintered microstructures were obtained. The high densities measured are caused by the substitution of Sn^{4+} ions for Co^{2+}, Co^{3+} and Zn^{2+} as established in previous works.[5,6] Samples doped with Co_3O_4 showed the higher density values and a better grain growth.

The occurrence of a secondary phase precipitated in the SCNF system is observed in the SEM image, and its composition consisting mainly of Sn and Co is confirmed by the EDS spectra included in Fig. 1. It can also be seen that the grains are mostly composed of SnO_2. In contrast, no secondary phases, neither segregated nor precipitated, where detected by SEM on the SZNF system (Fig. 2).

Further significant results were achieved by TEM, and the micrographs obtained with their respective EDS analysis, are shown in Figs. 3 and 4. As shown in Fig. 3, precipitates of different composition and smaller in size to those observed by SEM are present in the SCNF system. These novel precipitates formed during the sintering process do concentrate the additives and are very rich in Fe, the trivalent element added to improve the non-linear properties of the device.[12] Analogue precipitates to those detected in the SCNF system by TEM are observed in the SZNF system, though in a lesser extent, as shown in Fig. 4.

The acquisition of dark-field images and electron diffraction patterns of selected areas (SAD) of the various phases encountered was essential for the phase identification procedures. As shown in Fig. 5a and b, electron diffraction patterns of well crystallised structures were obtained. The diffraction pattern for the grain region (Fig. 5a) of both SCNF and SZNF samples evidenced a rutile type structure

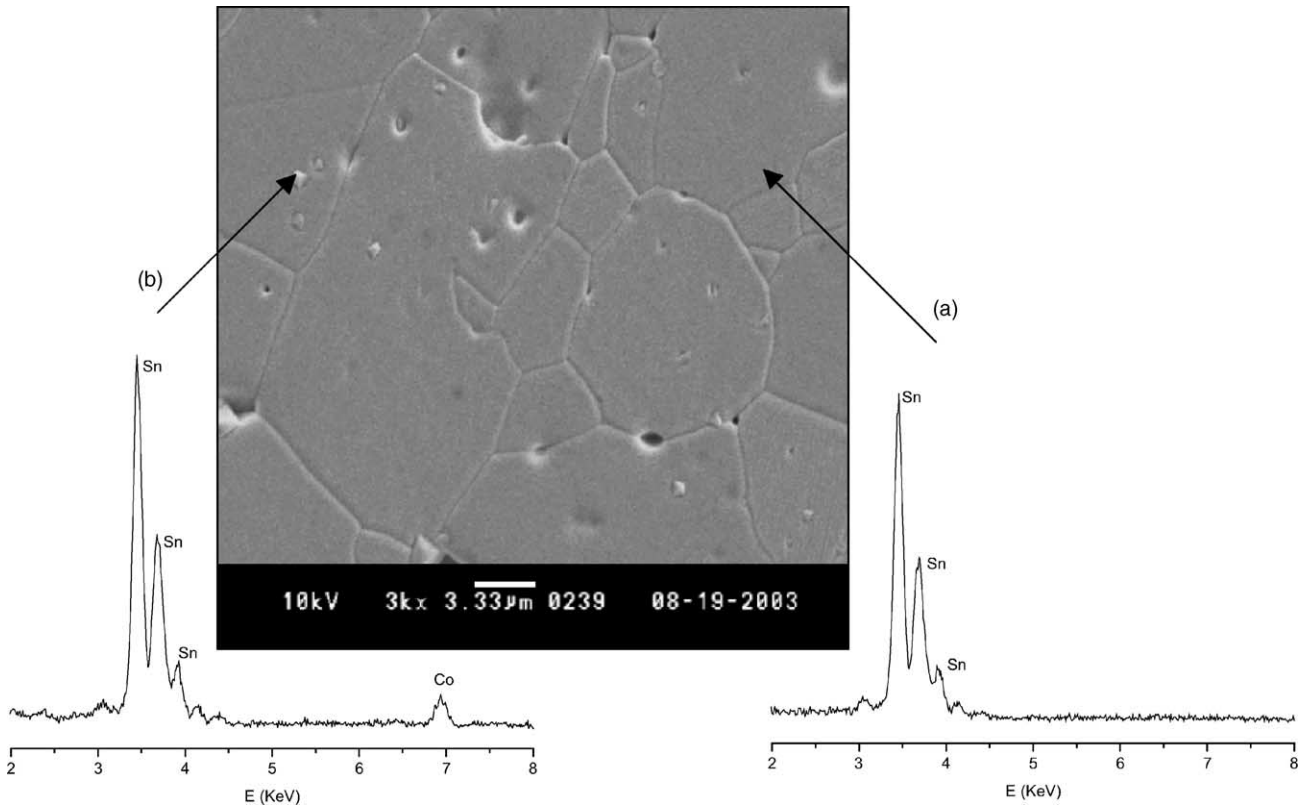

Fig. 1. SEM microstructure of the SCNF system and EDS analysis of: (a) grain region and (b) precipitates.

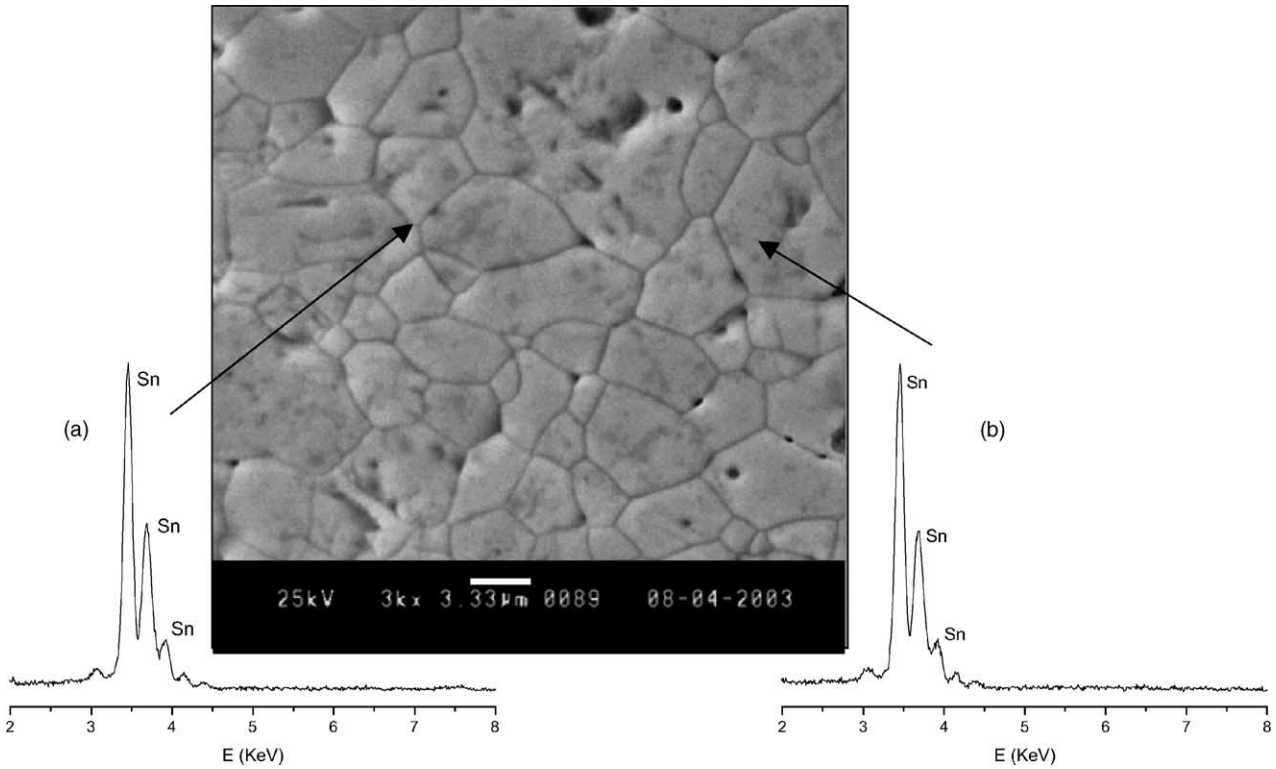

Fig. 2. SEM microstructure of the SZNF system and EDS analysis of: (a) boundary and (b) grain regions. No precipitates are observed.

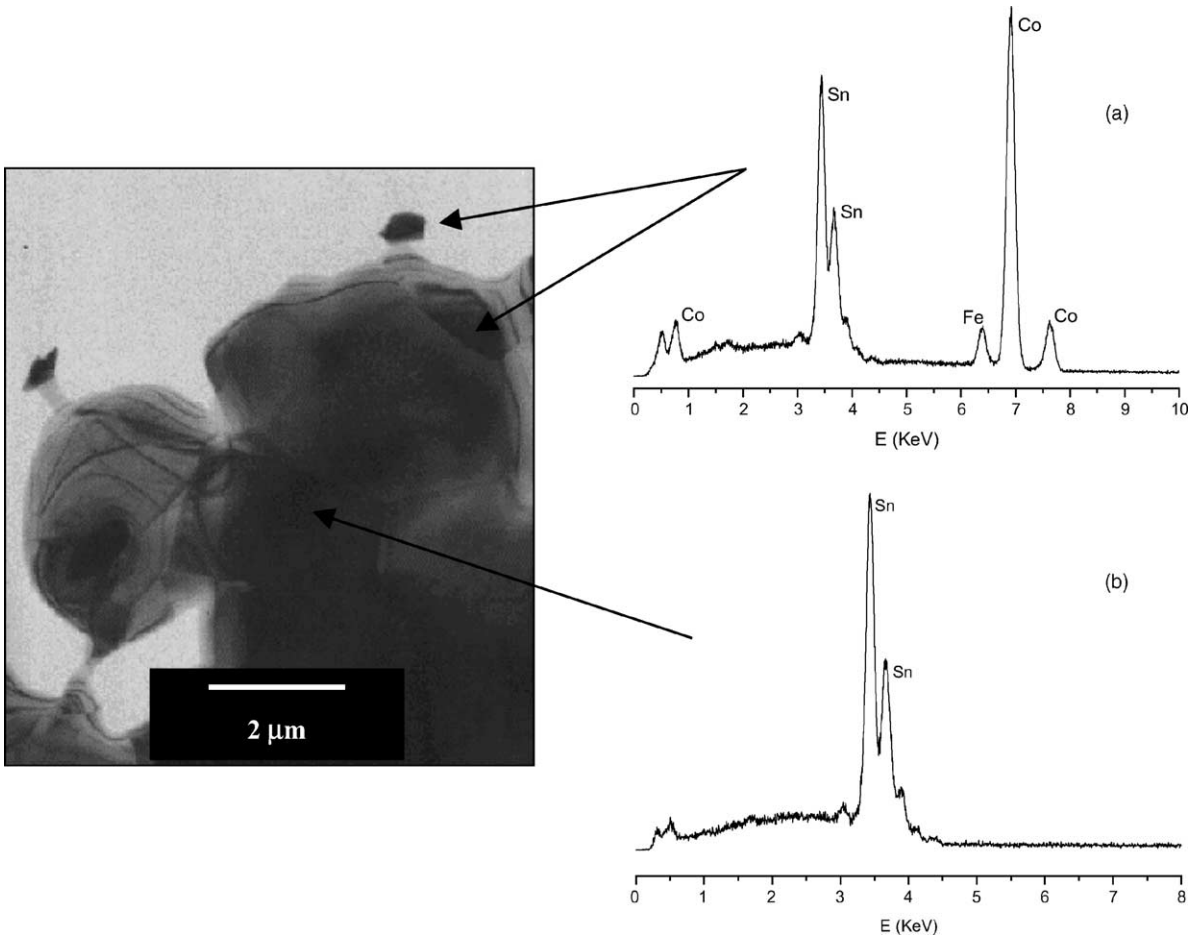

Fig. 3. TEM image and EDS analysis of the SCNF system: (a) precipitates and (b) grain region.

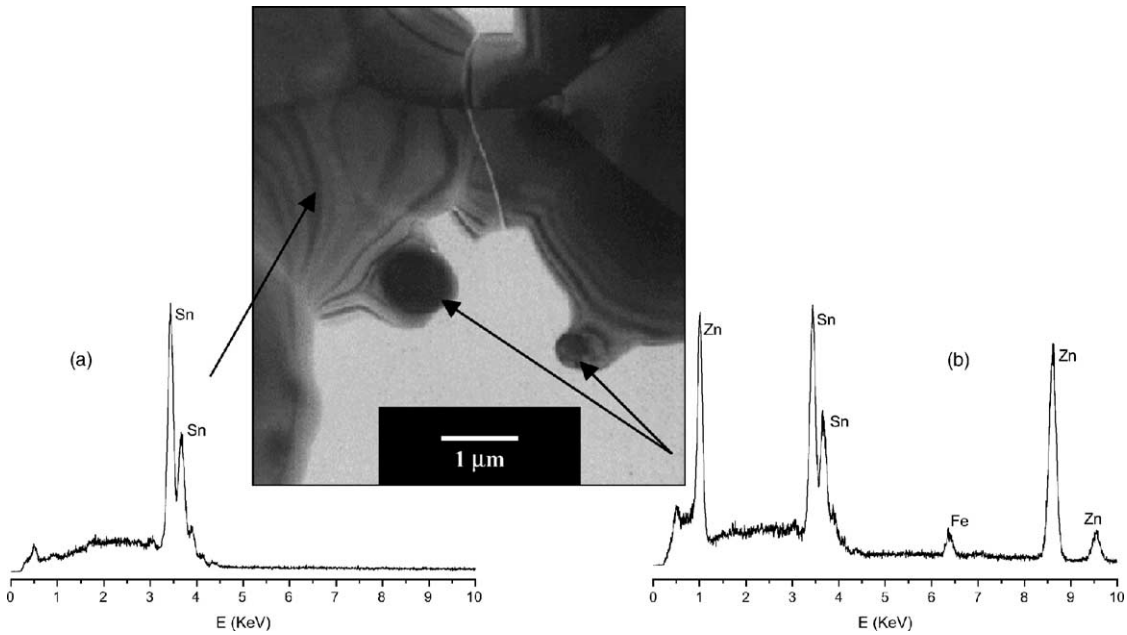

Fig. 4. TEM image and EDS analysis of the SZNF system: (a) grain region and (b) precipitates.

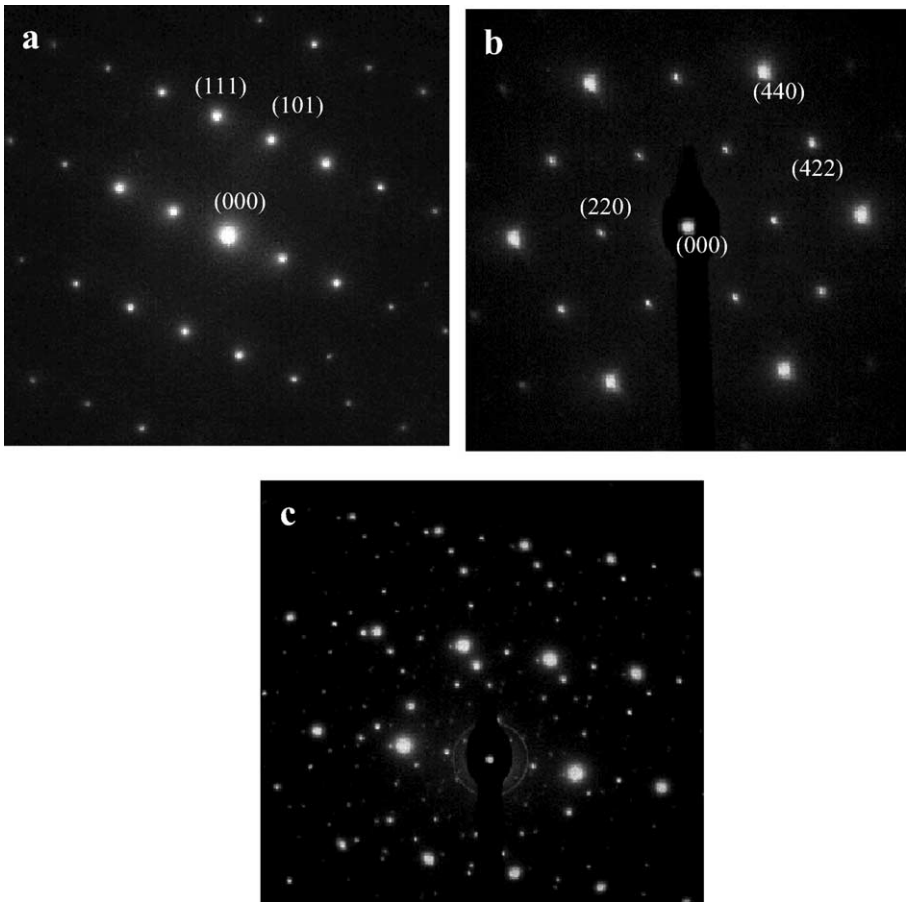

Fig. 5. (a) SAD pattern of the grain region matching for SnO_2; (b) SAD pattern of a precipitate in SCNF matching for $Co_{1.5}FeSn_{0.5}O_4$; (c) SAD pattern of a multi-phase particle in SZNF.

corresponding to SnO_2, whereas the second phase found in the SCNF system (Fig. 5b) was identified as $Co_{1.5}FeSn_{0.5}O_4$ in agreement with JCP-DS files.[13] This is a cubic symmetry phase with a unit cell parameter of 8.53 Å, whose composition is also supported by the EDS spectrum in Fig. 3. It was not possible to definitely identify the second phases that showed up in the SZNF sample for they do not correspond to single phases. Nevertheless, the high concentration of Zn and Sn observed in the EDS analysis, and the study of Fig. 5c and its resemblance to the cubic system Zn_2SnO_4 found in JCP-DS records,[14] lead to the assumption of Zn_2SnO_4 as one of the phases present in such precipitates.

Due to the special interest in the structure and composition of grain boundaries for they are believed to control the non-linear current–voltage characteristics, it is necessary to mention that the secondary phases are localised both inside the grains and grain boundaries, as well as in triple points.

The electrical properties of the samples were also studied and the *J–F* characteristic curves are shown in Fig. 6. The addition of Fe_2O_3 to the $SnO_2{\cdot}Co_3O_4{\cdot}Nb_2O_5$ ($\alpha = 4$) and to the $SnO_2{\cdot}ZnO{\cdot}Nb_2O_5$ ($\alpha = 7$) varistor systems highlighted their non-linear properties yielding values for the non-linear coefficient α of 25 and 9, respectively. These results corroborate the findings of Antunes et al.[11] who achieved acceptable α values with the addition of iron oxide to a $SnO_2{\cdot}CoO{\cdot}Nb_2O_5$ system. The segregation of Fe_2O_3 next to the grain boundary creates positive and negative defects, dominating the depletion layer and the grain-grain

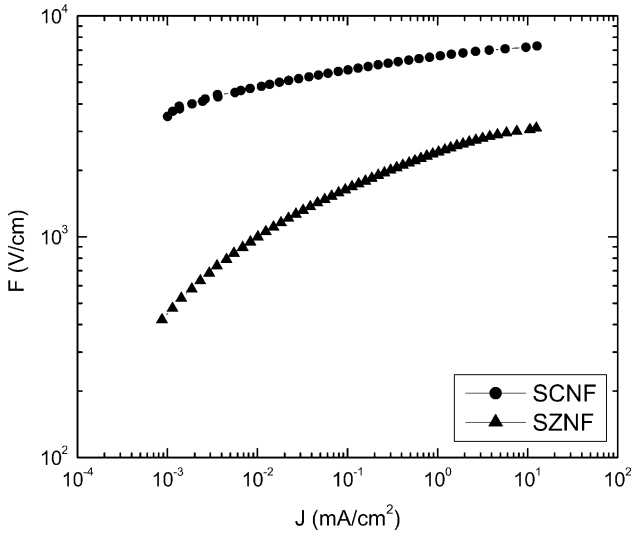

Fig. 6. *F* vs. *J* characteristic curves for the varistor systems SCNF and SZNF sintered at 1300 °C for 2 h.

interface, respectively, involved in the potential barrier formation. The viewed affinity of iron towards the formation of compounds with tin and cobalt or zinc oxides, may be a factor of relevance in the availability of Fe_2O_3 to be segregated to grain boundary regions and, moreover, an indication of its low solubility in the SnO_2 lattice. Thereafter, the lower α value found for the SZNF system might be ascribed to a minor segregation of Fe^{3+} species to grain boundaries.

4. Conclusions

The experimental results reported in this paper lead to the following conclusions:

1. The occurrence of secondary phases, in view of the reactivity and low solubility of the foreign species in the SnO_2 lattice, was evidenced and studied with transmission electron microscopy and found to occur inside the grains and at grain boundaries in samples with the addition of iron, niobium and cobalt or zinc oxides.
2. Electron diffraction patterns of selected areas and EDS analysis allowed to identify the secondary phase encountered in the microstructure of SCNF samples as the cubic system $Co_{1.5}FeSn_{0.5}O_4$.
3. In samples containing ZnO only small particles of secondary phases were found through TEM analysis. Electron diffraction patterns of selected areas revealed their multi-phase nature.
4. The addition of Fe_2O_3 to SnO_2-based varistors enhances the non-linear properties as it segregates to the grain boundaries.
5. Although the presence of precipitated phases at grain boundaries is believed to modify the electrical properties of the devices, actually, their influence on the overall varistor behaviour seems to be of minor importance. We conclude that the non-ohmic properties are controlled by grain–grain junctions with transition metals segregated at grain boundary regions.

Acknowledgements

The authors express their thanks to the Programa CYTED (Proyecto PI-VIII.13 PROALERTA), to ANPCyT and to Fundación Antorchas (Argentina), to CNPq and FAPESP (Brazil) for their financial support.

References

1. Matsuoka, M., Progress in research and development of zinc oxide varistors. In *Grain Boundary Phenomena in Electronic Ceramics, Advances in Ceramics, Vol 1*, ed. L. M. Levinson. The American Ceramic Society Inc., Ohio, 1981, pp. 290–308.
2. Levinson, L. M. and Philipp, H. M., Zinc-oxide varistors—a review. *Am. Ceram. Soc. Bull.* 1996, **85**, 639–646.
3. Gupta, T. K., Application of zinc oxide varistors. *J. Am. Ceram. Soc.* 1990, **73**, 1818–1840.
4. Castro, M. S. and Aldao, C. M., Thermionic, tunelling and polarization currents in zinc oxide varistors. *J. Eur. Ceram. Soc.* 1997, **17**, 1533–1537.
5. Fayat, J. and Castro, M. S., Defect profile and microstructural development in SnO_2-based varistors. *J. Eur. Ceram. Soc.* 2003, **23**, 1585–1591.
6. Pianaro, S. A., Bueno, P. R., Longo, E. and Varela, J. A., A new SnO_2-based varistor system. *J. Mater. Sci. Lett.* 1995, **14**, 692–694.
7. Oliveira, M. M., Soares, Jr. P.C., Bueno, P. R., Leite, E. R., Longo, E. and Varela, J. A., Grain boundary segregation and precipitates in La_2O_3 and Pr_2O_3 doped SnO_2·CoO-based varistors. *J. Eur. Ceram. Soc.* 2003, **23**, 1875–1880.
8. Bueno, P. R., Leite, E. R., Oliveira, M. M. and Orlandi, M. O., Role of oxygen at the grain boundary of metal oxide varistors: a potential barrier formation mechanism. *Appl. Phys. Lett.* 2001, **79**, 48–50.
9. Pianaro, S. A., Bueno, P. R., Longo, E. and Varela, J. A., Microstructure and electric properties of a SnO_2 based varistor. *Ceram. Int.* 1999, **25**, 1–6.
10. Williams, D. B. and Carter, C. B., *Transmission Electron Microscopy: a Text Book for Materials Science*. Plenum Press, New York, 1996.
11. Mendelson, M. I., Average grain size in polycrystalline ceramics. *J. Am. Ceram. Soc.* 1969, **52**, 443.
12. Antunes, A. C., Antunes, S. R. M., Zara, A. J., Pianaro, S. A., Longo, E. and Varela, J. A., Effect of Fe_2O_3 doping on the electrical properties of SnO_2 based varistors. *J. Mater. Sci.* 2002, **37**, 2407–2411.
13. JCP-DS file number 30-0445.
14. JCP-DS file number 73-1725.